NASA TECHNICAL MEMORANDUM

NASA TM X-52367

NASA TM X-52367

GPO PRICE $ _____

CFSTI PRICE(S) $ _____

Hard copy (HC) 3.00

Microfiche (MF) _____

ff 653 July 65

ACOUSTIC LINER STUDIES AT THE LEWIS RESEARCH CENTER

by Bert Phillips
Lewis Research Center
Cleveland, Ohio

TECHNICAL PAPER presented at Fourth Combustion Conference
sponsored by the Interagency Chemical Rocket Propulsion Group
Menlo Park, California, October 2-13, 1967

NATIONAL AERONAUTICS AND SPACE ADMINISTRATION · WASHINGTON, D.C. · 1967

ACOUSTIC LINER STUDIES AT THE LEWIS RESEARCH CENTER

by Bert Phillips

Lewis Research Center
Cleveland, Ohio

TECHNICAL PAPER presented at

Fourth Combustion Conference sponsored by the
Interagency Chemical Rocket Propulsion Group
Menlo Park, California, October 2-13, 1967

NATIONAL AERONAUTICS AND SPACE ADMINISTRATION

ACOUSTIC LINER STUDIES AT THE LEWIS RESEARCH CENTER

by Bert Phillips

Lewis Research Center
National Aeronautics and Space Administration
Cleveland, Ohio

INTRODUCTION

Research on acoustic liners at the Lewis Research Center was prompted by the original work of Wanhainen (ref. 1), presented at the 1966 ICRPG meeting, which indicated a lack of understanding of mean flow and high wave amplitude effects on liner behavior. The research has taken two approaches: the testing of arrays of isolated Helmholtz resonators in a rocket engine and the cold flow testing of a single Helmholtz resonator. The purposes of the "hot" testing were to determine whether mean flow effects should be included in a calculation of the cavity resonant frequency and to determine the most effective axial position of an acoustic liner. The purpose of the cold flow testing was to determine the effects of mean flow and high wave amplitude on the resonator behavior. The "hot testing" will be discussed first.

Testing of Arrays of Helmholtz Resonators in a Rocket Engine. The "hot testing" was conducted in a 300 psi chamber pressure, 11-inch diameter, hydrogen-oxygen rocket engine with a nominal sea level thrust of 20,000 pounds. A sketch of the array of resonators is shown in figure 1. There were 8 rows by 34 resonators per row. The holes were spaced on a 1-inch square array with the first row 3/4-inch from the injector face. Each cavity depth could be varied from one run to the next and provision was made for resonator cavity gas temperature measurement and cavity gas sampling.

A typical test is shown in figure 2. Each liner configuration is stability rated by decreasing the inlet hydrogen temperature while holding the O/F and P_c constant. The flush mounted high frequency transducer shows a low amplitude signal which increases until, at some H_2 inlet temperature, transition to full-scale instability, or screech, is encountered. The difference in transition temperature between a baseline (no liner) configuration and the liner configuration is taken as a measure of the liner damping (i.e. the lower the transition temperature, the higher the damping).

Shown in figure 3 is a plot of the reduction in H_2 inlet temperature versus cavity depth for the entire array. The cavity depth corresponding to a reduction in temperature of 47° corresponds to the tuning of the cavity resonant frequency with the wave frequency. The wave frequency corresponds to the frequency of the pretransition oscillation and is obtained by spectral analysis of the high frequency transducer output. A sample of the spectral analysis is shown in figure 4a. For comparison, a spectral analysis of the full-scale instability is shown in figure 4b. The full-scale instability exists in both the 1T mode (3300 Hz) and the 2T mode (5700 Hz). It is not possible to determine the modal type for the pretransition oscillation, but the difference in frequency can be noted.

By measuring the cavity gas temperatures and compositions at transition, a cavity resonant frequency, based on available correlations from reference 2, and the cavity depths of figure 3, can be calculated. These results are shown in figure 5. The spread in calculated frequencies is due to variations in the measured cavity gas temperature before transition to full-scale instability. On the same plot is shown the wave frequency based on spectral analysis of the pretransition noise. In order for the cavity depth of 1-3/4 inches (from fig. 3) to have the maximum damping, the resonant frequency must have been equal to the wave frequency, thus, the frequency calculation is in error by the difference between 4400 and 6600 Hertz or, a frequency shift factor of 0.66 is required. In order to account for such a frequency shift, recourse is made to the frequency shift correlation of reference 3 which is based on mean chamber flow. This correlation, modified for Mach number, is shown in figure 6. The contraction ratio of the rocket engine used was 1.9 which corresponds to a Mach number of 0.33 which, in turn, corresponds to a frequency shift ratio of 0.63. The agreement between the required and mean flow frequency shifts indicates that a mean flow effect is required for calculating the cavity resonant frequency.

In order to determine the most effective axial position for a liner, a series of tests were conducted with the rows nearest the injector. The first row tested was that nearest the injector (3/4-inch) and the results are shown in figure 7. The reduction in hydrogen inlet temperature is plotted versus calculated cavity resonant frequency for just the first row alone (circular symbols). As the next row, and even the next two rows were added, there was no additional decrease in the transition temperature within experimental error, indicating that it was the first row alone that contributed to the damping. Thus, a liner consisting of one row of holes 3/4-inch from the injector face would be required for this engine configuration.

Cold Flow Testing. The apparatus for determining mean flow and high wave amplitude effects is shown in figure 8. It consists of a small air wind tunnel on which were mounted electrical and electropneumatic sirens for sound sources. The Helmholtz resonator was flush mounted with the inside of the tunnel as shown and the air flow was measured by a pitot static probe tube. The system was limited to 360 ft/sec maximum flow velocity and 165 db sound pressure level.

A detailed sketch of the Helmholtz resonator is shown in figure 9. The aperture thickness and area could be readily varied and the cavity depth was also variable. The effects of flow and wave amplitude were determined by fixing the flow and/or wave amplitude and measuring the oscillating phase and pressure on both sides of the aperture as the cavity depth was varied. From these determinations, the resonator aperture resistance and reactance could be readily calculated.

A typical experiment was to determine the reactive mass or aperture effective length from the phase measurements. In order to verify that the phase measurements were reliable, calibration tests were made by measuring test chamber SPL and phase as the cavity depth was varied for fixed siren power and frequency. The results are shown in figure 10.

As the cavity depth was varied, cavity resonant frequency also varied. At the tuned point, the test chamber SPL reached a minimum when the phase angle was 90°, thus indicating that phase measurement could be used to determine tuning and aperture reactance.

The effects of mean flow on aperture reactive mass, as expressed by the reduction in this aperture effective length, is shown in figure 11. Two aperture thicknesses and three frequencies were tested and there was no affect of either frequency or thickness in the ranges tested. On the same plot, a line representing the l_{eff}, correction factor, is shown. When the reduction in l_{eff} (Δl_{eff}) equals the l_{eff} correction factor, the l_{eff} is equal to the aperture thickness.

Comparison of the mean flow results with the results of figure 3 is shown in figure 12. The results, although qualitatively the same, are quantitatively different. The difference may be ascribed to variations in the turbulence level between the apparatus of reference 3 and the present experiment and the fact that the results of reference 3 represent tests with an array of connected resonators (acoustic liner) whereas the present experiment involved a single resonator. In any case, the results indicate that, at high flow rates, much of the l_{eff} is dissipated, or reduced to the aperture thickness. Thus, an initial design for a liner that will operate in a high velocity environment would be to set the l_{eff} equal to t, the aperture thickness.

The effect of mean flow on the aperture acoustic resistance is given in figure 13. The circular symbols, representing the data of reference 3, were obtained from the bandwidth of the absorption-frequency curves shown in figure 4 of that reference. The results show surprisingly good agreement.

The effect of wave amplitude on the aperture acoustic resistance is shown in figure 14. The results are plotted as ϵ, the nonlinear resistance parameter, versus the wave amplitude. The data does not seem to match the results reported by Pratt and Whitney, Blackman (ref. 2), or Ingaard (ref. 3).

Rather than plot the results as ϵ, the resistance was plotted directly versus the calculated acoustic particle velocity, as suggested by Ingaard in reference 4. This is shown in figure 15. The data agree with the equation $R = \rho v'$ where ρ is the gas density and v' is the calculated acoustic particle velocity. These results agree with reference 5 which attributes nonlinear acoustic resistance to a $\rho v'^2$ jet loss. This method of calculating the acoustic resistance should have great utility in simplifying liner design calculations.

The research at the Lewis Research Center is continuing with the purpose of applying the experimental cold flow technique discussed in this paper to a rocket engine environment. A preliminary test result is shown in figure 16. The engine is operated in a pretransition region at steady-state conditions. The cavity depth is increased while the oscillating pressures on both sides of the aperture are measured. The cavity is also purged with helium to define the cavity composition and temperature. From these results, the effects of chamber flow and wave amplitude on the resonator behavior can be determined.

REFERENCES

1. Wanhainen, John P.; Bloomer, Harry E.; and Vincent, David W.: Experimental Investigation of Acoustic Liners to Suppress Screech in Hydrogen-Oxygen Engines. Presented at the Third ICRPG Combustion Conference, Oct. 17-21, 1966.

2. Blackman, A. W.: Effect of Nonlinear Losses on the Design of Absorbers for Combustion Instabilities. ARS J., vol. 30, no. 11, Nov. 1960, pp. 1022-1028.

3. Mechel, F.; Mertens, P.; and Shilz, W.: Research on Sound Propagation in Sound - Absorbent Ducts with Superimposed Air Streams. Vol. III. Göttingen Univ. (West Germany) (AMRL-TDR-62-140, vol. III, DDC No. AD-296984), Dec. 1962.

4. Ingard, Uno: On the Theory and Design of Acoustic Resonators. J. Acoust. Soc. Am., vol . 25, no. 6, Nov. 1953, pp. 1037-1061.

5. Harrje, David T.; and Sirignano, William A.: Nonlinear Aspects of Combustion Instability in Liquid Propellant Rocket Motors. Rep. No. 553-F (NASA CR-77672), Princeton Univ., June 1, 1966, p. 38.

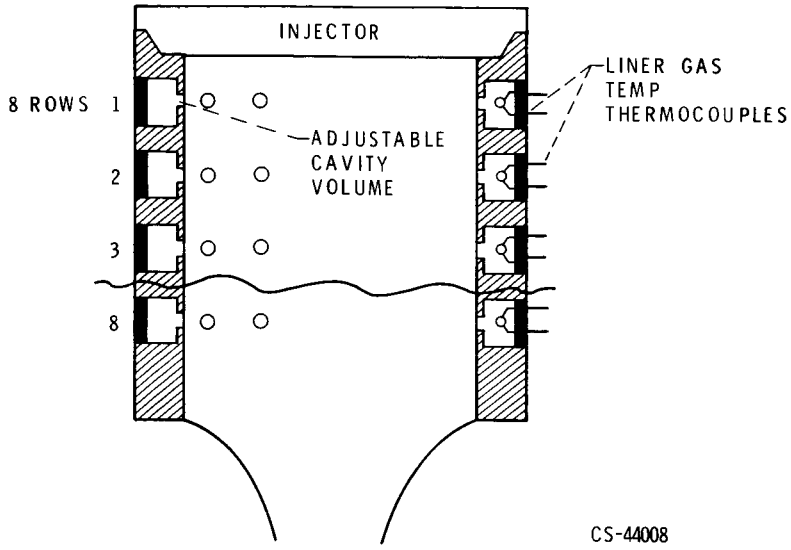

Figure 1. - Tunable liner.

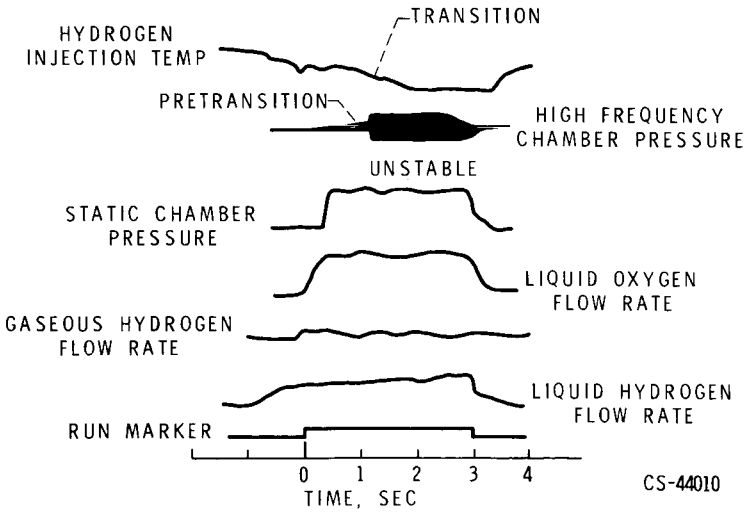

Figure 2. - Typical screech rating test.

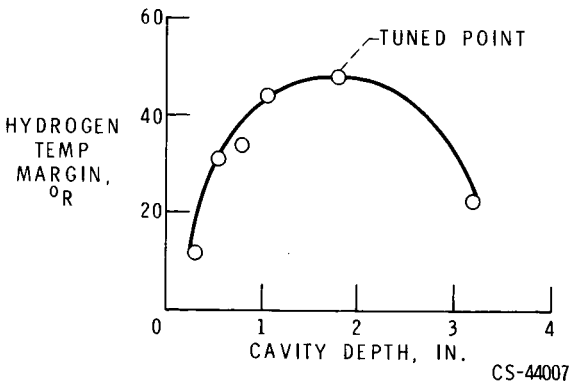

Figure 3. - Hydrogen temperature margin vs liner cavity depth.

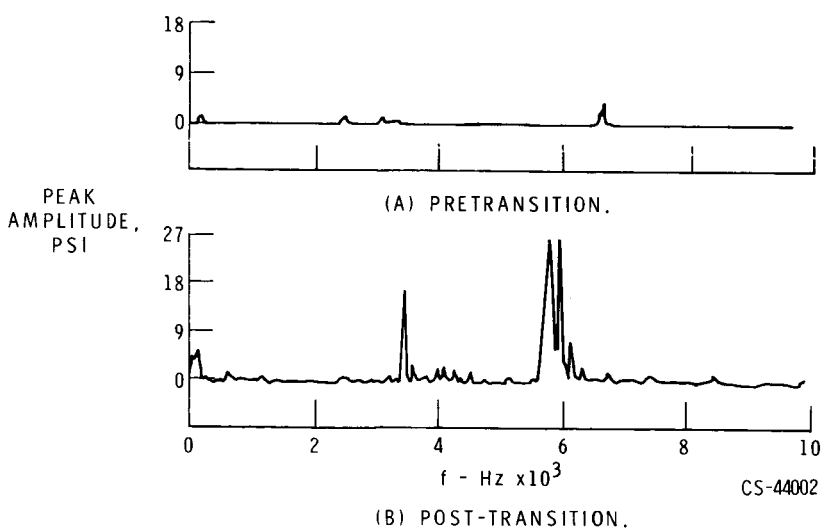

Figure 4. - Amplitude spectral analyses of high frequency transducer data.

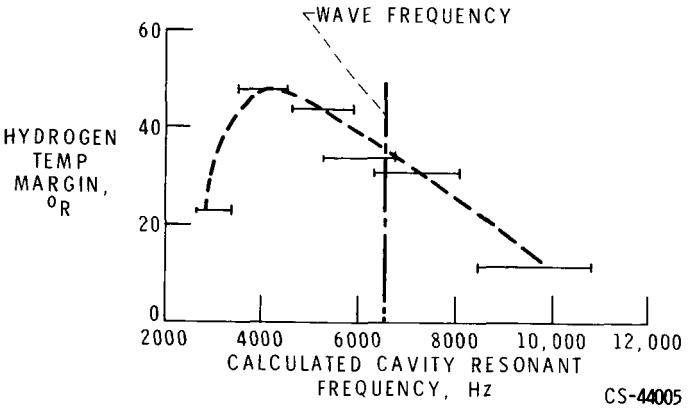

Figure 5. - Tuning curve for 8 row liner.

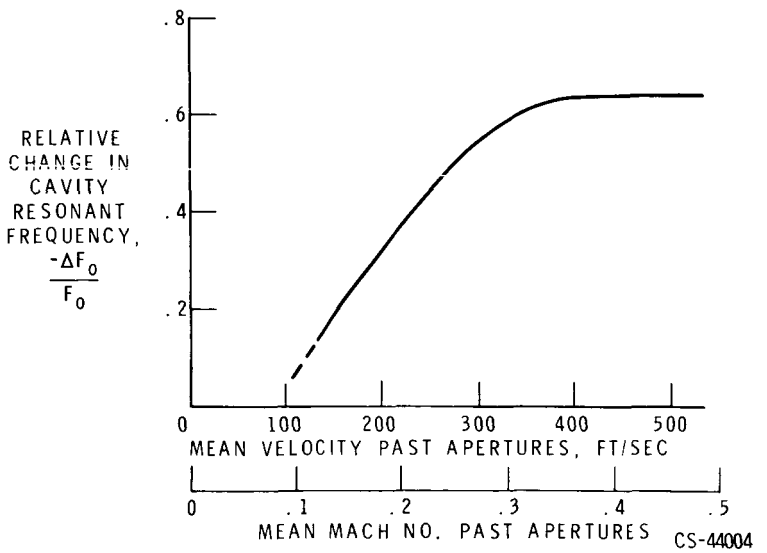

Figure 6. - Relative change in cavity resonant frequency vs mean flow past resonator apertures.

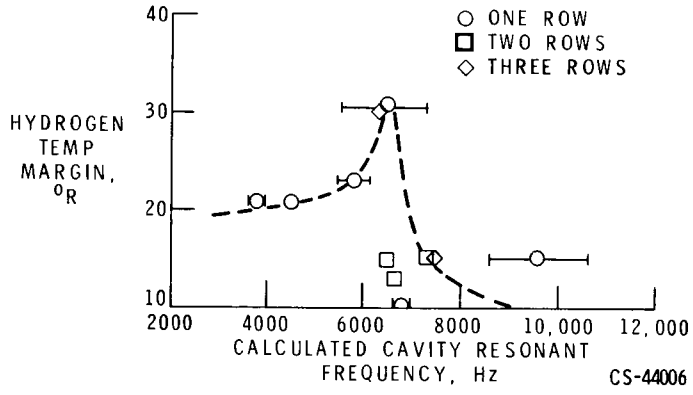

Figure 7. - Effect of liner length on stability.

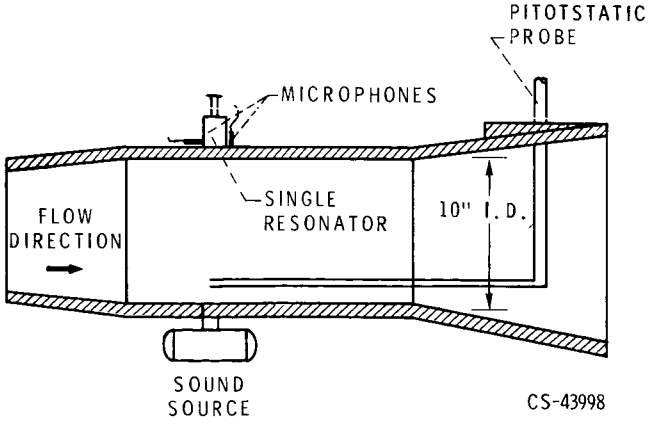

Figure 8. - Test section.

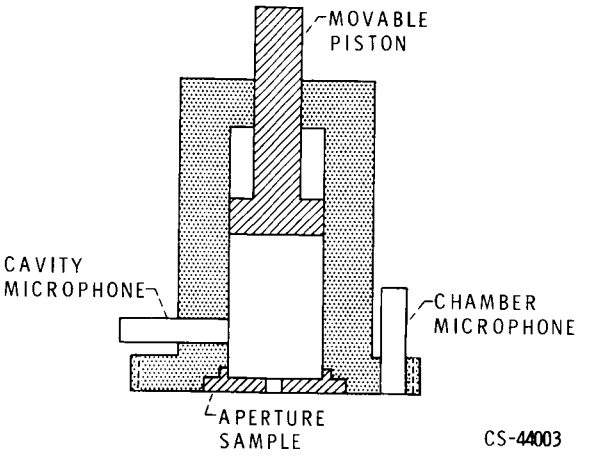

Figure 9. - Single resonator cross section.

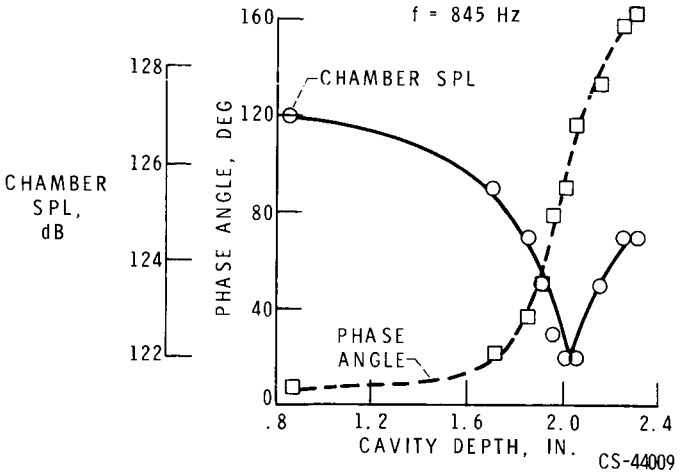

Figure 10. - Phase and SPL vs cavity depth.

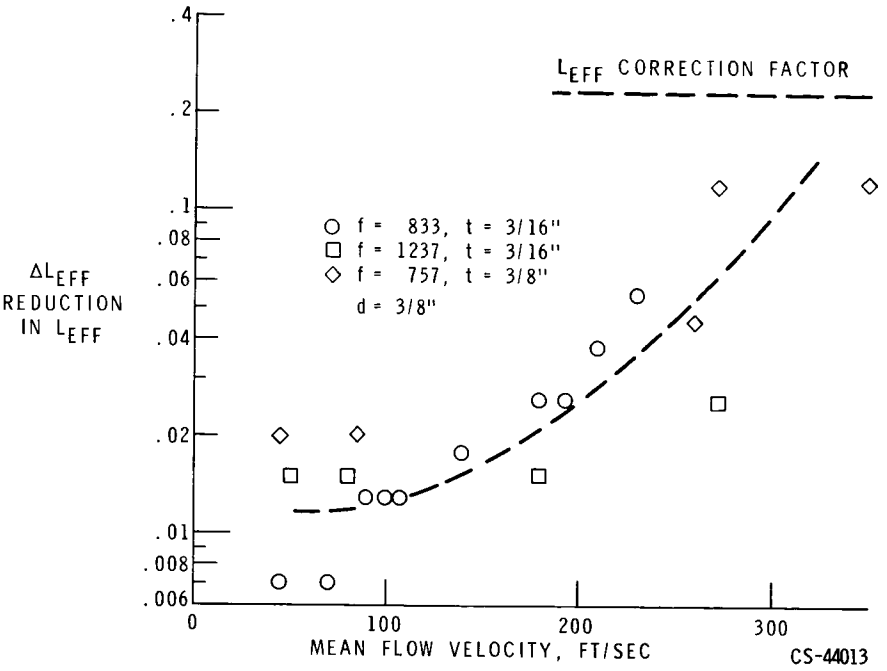

Figure 11. - L_{EFF} vs flow velocity.

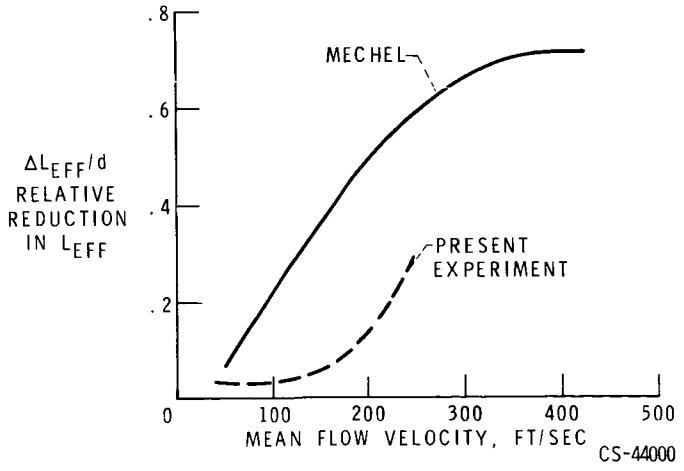

Figure 12. - Comparison of effect of flow on L_{EFF}.

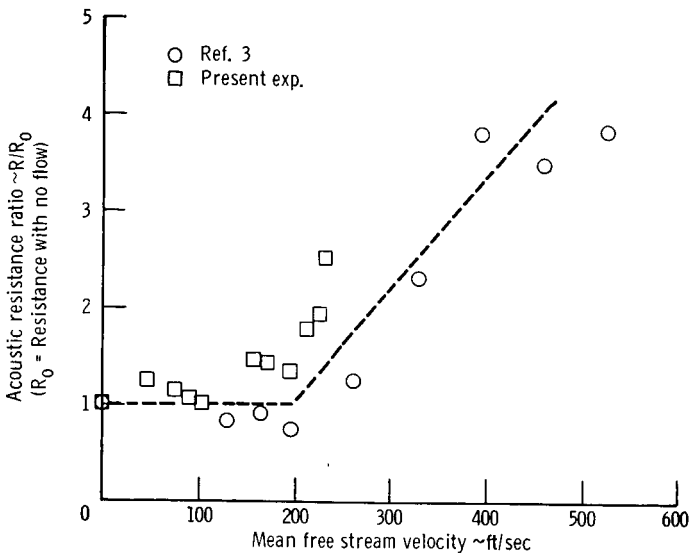

Figure 13. - Effect of mean flow on acoustic resistance.

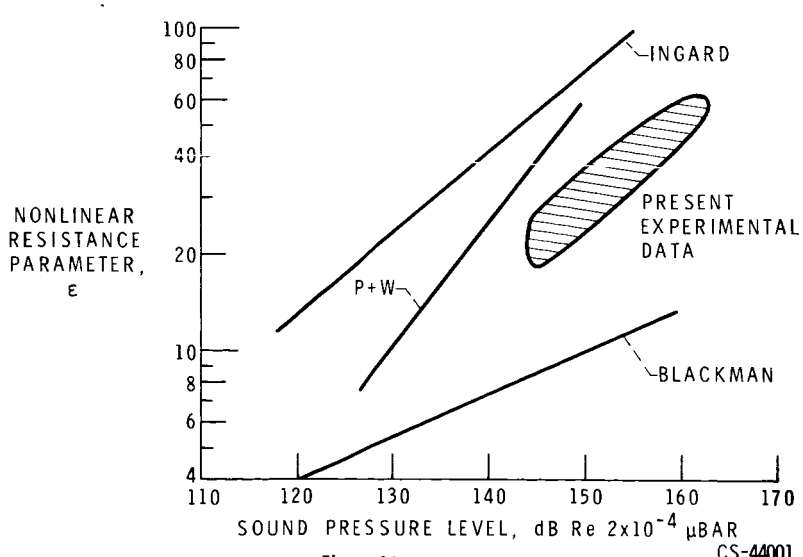

CS-44001

Figure 14. - ε vs sound pressure level.

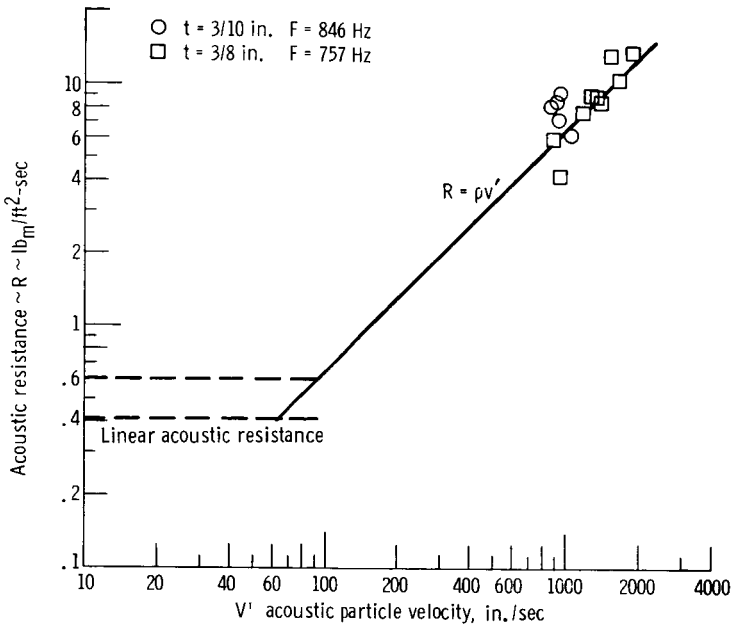

Figure 15. - Acoustic resistance vs acoustic particle velocity.

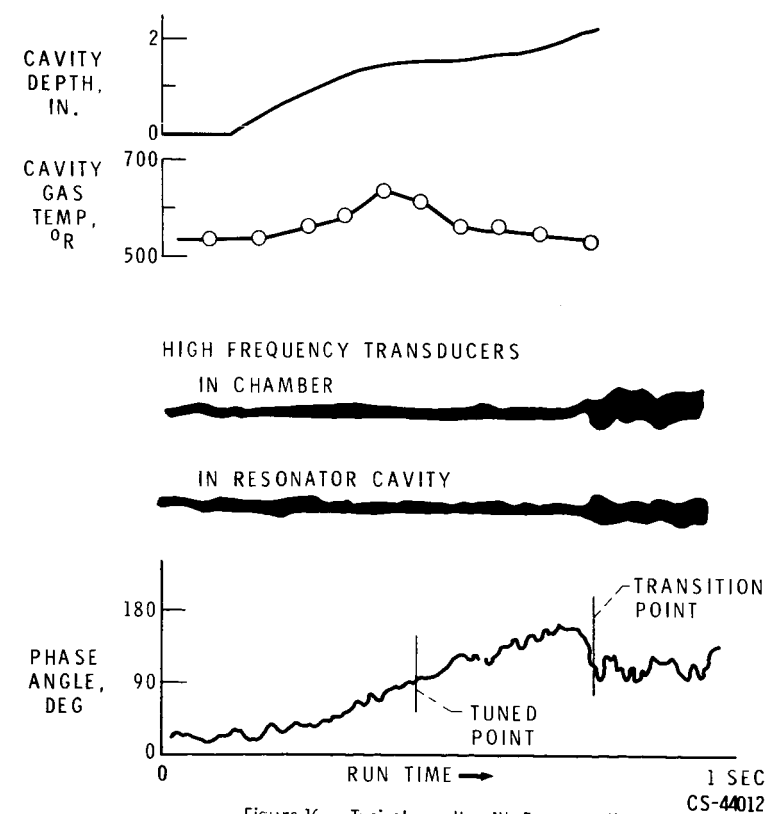

Figure 16. - Typical results with 5 - prong liner.